American Journal of Pathology, Vol. 147, No. 2, August 1995

Chemical and Immunological Heterogeneity of Fibrillar Amyloid in Plaques of Alzheimer's Disease and Down's Syndrome Brains Revealed by Confocal Microscopy

Marie Luise Schmidt, Kathryn Ann Robinson, Virginia M.-Y. Lee, and John Quinn Trojanowski

From The Department of Pathology and Laboratory Medicine, The University of Pennsylvania School of Medicine, Philadelphia, Pennsylvania

Amyloid β peptides (Aβ) are deposited in the brains of Alzheimer's disease (AD) and elderly Down's syndrome (DS) patients in a variety of amyloid plaques. Among these are classical plaques composed of a spherical core and a corona. Analyzing AD tissue sections single and double stained with anti-Aβ antibodies and thioflavin S (thioS) by bright field, fluorescence, and confocal microscopy revealed that spherical plaque cores consist of a thioS-positive center and an anti-Aβ antibody immunoreactive rim. This indicates that there is a fibrillar form of amyloid that is thioS positive but not immunoreactive with anti-Aβ antibodies. In contrast, classical plaques in DS patients have irregular cores that are thioS positive as well as anti-Aβ immunoreactive. In addition, a subset of plaques in both DS and AD patients have a distinct "fibrous" appearance when stained with thioS, but are amorphous when immunostained. These findings suggest that anti-Aβ antibodies and thioS stain similar, as well as different forms of fibrillar amyloid. Aβ may become thioS positive by interacting with one or more of its known molecular chaperons, and this may be important for the pathogenesis of AD, given that thioS-positive Aβ deposits are associated with neuritic and synaptic damage. (Am J Pathol 1995, 147:503–515)

Senile plaques are one of the diagnostic lesions in Alzheimer's disease (AD) brains, and β-amyloid (Aβ) peptides are the major components of the amyloid fibrils in all types of AD plaques. The Aβ peptides range in length from 39 to 42 amino acids, and these peptides are cleavage products of much larger amyloid precursor proteins.[1,2] However, there is considerable variation in the size of Aβ peptides due to heterogeneity in the amino and carboxyl terminal cleavage sites. Aβ appears to be produced by a normal proteolytic pathway *in vivo* and *in vitro*.[3–9] Whether Aβ accumulates in the brain because of impaired clearance mechanisms or as a result of modifications of Aβ itself remains to be determined. A variety of morphologically distinct types of Aβ deposits have been described in the brains of AD patients.[10–13] Diffuse plaques have been considered early lesions because they are not associated with dystrophic neurites, are the predominant type of Aβ deposits in the non-demented elderly, and are the first lesions detected in young Down's syndrome (DS) patients,[10,14–19] but see Ikeda et al.[12] Diffuse plaques are immunoreactive with a variety of different anti-Aβ antibodies, but they generally do not stain with dyes that bind to amyloid such as Congo red and thioflavin S (thioS).[10,20] On the other hand, more complex amyloid plaques termed neuritic, classical, and compact plaques are considered to be more "mature," and they are thioS positive and are immunostained with anti-Aβ antibodies.[10,21–23] These plaques also contain additional proteins (eg, α1-antichymothrypsin, apolipoprotein E, complement proteins, etc.) and cellular elements (eg, astrocytic processes, dystrophic neurites, microglia, neurons with and without neurofibrillary tangles). Hence, these plaques are far more complex than diffuse plaques, which do not appear to correlate with the severity of the dementia in AD.

To examine the chemical and immunocytological heterogeneity of amyloid in these complex plaques,

Supported by grants by the National Institute of Aging.

Accepted for publication May 5, 1995.

Address reprint requests to Marie L. Schmidt, Ph.D., Department of Pathology and Laboratory Medicine, University of Pennsylvania School of Medicine, Maloney Bldg. Basement Rm. A009, 3400 Spruce Street, Philadelphia, PA 19104–4283.

Table 1. *Patient Demographic Information*

Patient no.	Diagnosis	Age (years)	Postmortem interval (hours)	Tissue sections
1	AD	73	2.5	Frozen
2	AD	76	7.5	Frozen
3	AD/PD*	84	7	Frozen
4	AD	86	7	Frozen
5	AD	56	5	Paraffin
6	AD	71	10	Paraffin
7	AD	73	6	Paraffin
8	AD	74	6	Paraffin
9	AD	77	5	Paraffin
10	AD	80	5	Paraffin
11	AD	80	17	Paraffin
12	AD	81	17	Paraffin
13	AD	81	19	Paraffin
14	AD	82	13	Paraffin
15	AD	84	17	Paraffin
16	AD	89	14	Paraffin
17	DS	53	10	Paraffin
18	DS	54	14	Paraffin
19	DS	57	6	Paraffin
20	DS	58	13	Paraffin
21	DS	61	5	Paraffin, Frozen
22	DS	64	14	Paraffin
23	DS	67	36	Paraffin

*Alzheimer's and Parkinson's diseases.

Table 2. *Specificity and Source of Antibodies*

Antibody	Species	Mono-/Poly-clonal	Antigen	Dilution	Source	Reference
Frozen tissue						
2332	Rabbit	Poly	Aβ	1:6000	Athena*	26
10D5	Mouse	Mono	NH2-Aβ	1:50	Athena	49
T46	Mouse	Mono	tau (aa404–441)	Neat	Lee	50
T3P	Rabbit	Poly	PHF-tau (aa 389–402)	1:100	Lee	50
PHF1	Mouse	Mono	PHF-tau (S396/404)	1:200	S. Greenberg	51
Paraffin-embedded tissue						
UP107	Rabbit	Poly	Aβ	1:2000	B. Greenberg	52
2332	Rabbit	Poly	Aβ	1:16000	Athena	26
SP28	Rabbit	Poly	Aβ (β-turn)	1:8000	B. Frangio	53

This table lists the antibody designations, the species in which each was raised, whether the antibody is mono- or polyclonal, the antigen each recognized, the dilution at which each antibody was used in this study, the source, eg, commercial source or the person who provided each antibody, and a reference that contains information pertaining to its specificity. The following abbreviations were used: aa = amino acid sequence, Aβ = amyloid protein, NH2-Aβ = amino terminus of Aβ protein, PHF = paired helical filament, S = serine.
* San Francisco, CA.

we used brightfield, fluorescence, and confocal microscopy to study the relationship of thioS-positive and anti-Aβ-immunoreactive components in these plaques in AD and DS brains. We found that the Aβ peptides in extracellular fibrillar amyloid deposits are immunologically heterogeneous, and this heterogeneity may have implications for the pathogenesis of the amyloidosis in the AD and DS brains.

Materials and Methods

Patient Information and Tissue Samples

Samples of the middle frontal gyri from 23 patients were used in this study. The diagnosis, age, postmortem interval, and tissue preparation for each sample are listed in Table 1. All patients had pathologically confirmed AD based on the consensus criteria of the National Institute on Aging.[24] Patient 3 had concomitant Parkinson's disease, and seven patients (nos. 17 to 23) were older individuals with Down's syndrome. Tissue blocks from the middle frontal gyri were collected at autopsy and immersed in 70% ethanol containing 150 mmol/L sodium chloride (ETOH/NaCl). Frozen and paraffin sections of the tissue samples were prepared as outlined below.

Preparation and Staining of Frozen Samples

Subsequent to overnight fixation in ETOH/NaCl, tissue blocks from some patients (nos. 1 to 4, 21) were

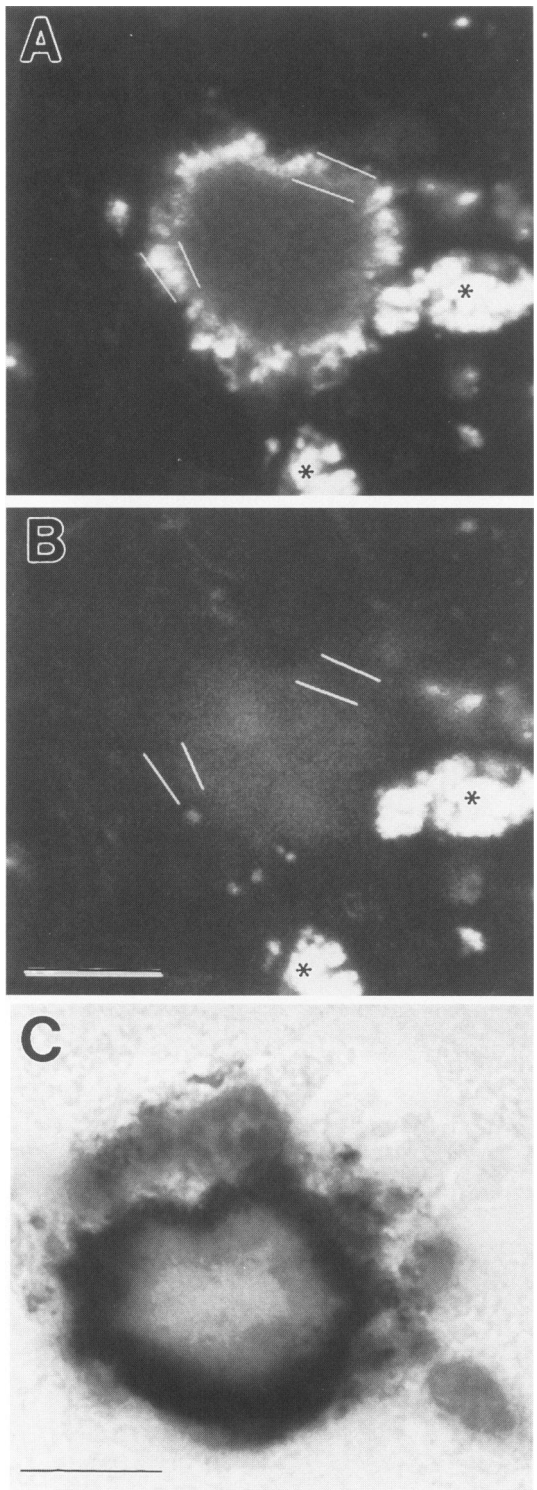

Figure 1. *This figure illustrates a spherical compact plaque in a frozen section of the frontal cortex of an AD patient that was immunostained with anti-Aβ antiserum 2332 and a TR-labeled secondary antibody.* (**A**) *depicts a single optical section through the center of a compact plaque obtained in the TR channel of the CLSM. Two pairs of lines were plotted as an overlay image using the Leica CLSM software to delineate portions of the strongly immunofluorescent rim of this plaque core. Lipofuscin autofluoresces in both the TR and the FITC channels, and two large lipofuscin accumulations are marked by asterisks.* (**B**) *A simultaneously acquired image by the second photomultiplier using FITC filters shows the autofluorescent center of the plaque core. The same overlay image was superimposed to indicate that the immunofluorescently stained rim of the core is located in the periphery of the autofluorescent center with no overlap between the two structures.* (**C**) *A 6 μm-thick paraffin section of the frontal cortex of an AD patient was immunostained with anti-Aβ antiserum 2332 and visualized with the PAP procedure using DAB as chromogen. Note the nearly unstained center similar to the one in* **A**. *Scale bar = 10 μm.*

immersed in 20% and 30% sucrose in phosphate buffered saline (PBS), pH 7.3 at 4°C. After sucrose infiltration, the tissue was embedded in ornithine carbamoyltransferase compound and frozen. 40 μm-thick frozen sections were cut and washed in PBS, to which 0.5% Triton X-100 (washing buffer) was added for 90 minutes. This and all of the following incubations and rinses were performed on a shaker. The tissue sections were then incubated for 90 minutes in blocking solution (ie, washing buffer with 2% horse serum). This was followed by incubation in the primary antibody diluted with blocking solution overnight at 4°C. Sections were washed three times for 15 minutes in washing buffer followed by incubation in a fluorescently labeled secondary antibody diluted in blocking solution overnight at 4°C. The sections were then washed in several changes of washing buffer for a total of 2 hours, followed by fixation in 4% neutral buffered formalin for 1 hour. Distilled water was used for each of the final three 15-minute rinses. Some sections were mounted onto glass slides, covered with Crystal Mount (Biomeda Corp., Foster City, CA) containing 35 mg dithioerythritol as antifade medium. The preparations were then dried on a heating plate set at 60°C and subsequently stored in the dark at room temperature. Other immunostained sections were covered with a glycerin-based antifade medium containing 5% *n*-propyl gallate, 0.25% 1,4-diazabicyclo-(2,2,2 octane), and 0.0025% paraphenylenediamine,[25] and coverslipped. Using this immunostaining protocol, we observed that antibodies completely penetrated 40 μm-thick tissue sections (see below and Figure 2C).

A description of the specificities of the primary antibodies and the dilutions used in this study are given in Table 2. Secondary fluorescently labeled antibodies were purchased from Jackson Immuno Research, (West Grove, PA). Donkey anti-rabbit or donkey anti-mouse secondary antibodies labeled with fluorescein isothiocyanate (FITC) or Texas red (TR) were used at dilutions of 1:600. Double-immunostained sections were prepared by incubating the sections with both primary antibodies simultaneously, and after the appropriate washes, incubating the sections again simultaneously with both secondary antibodies.

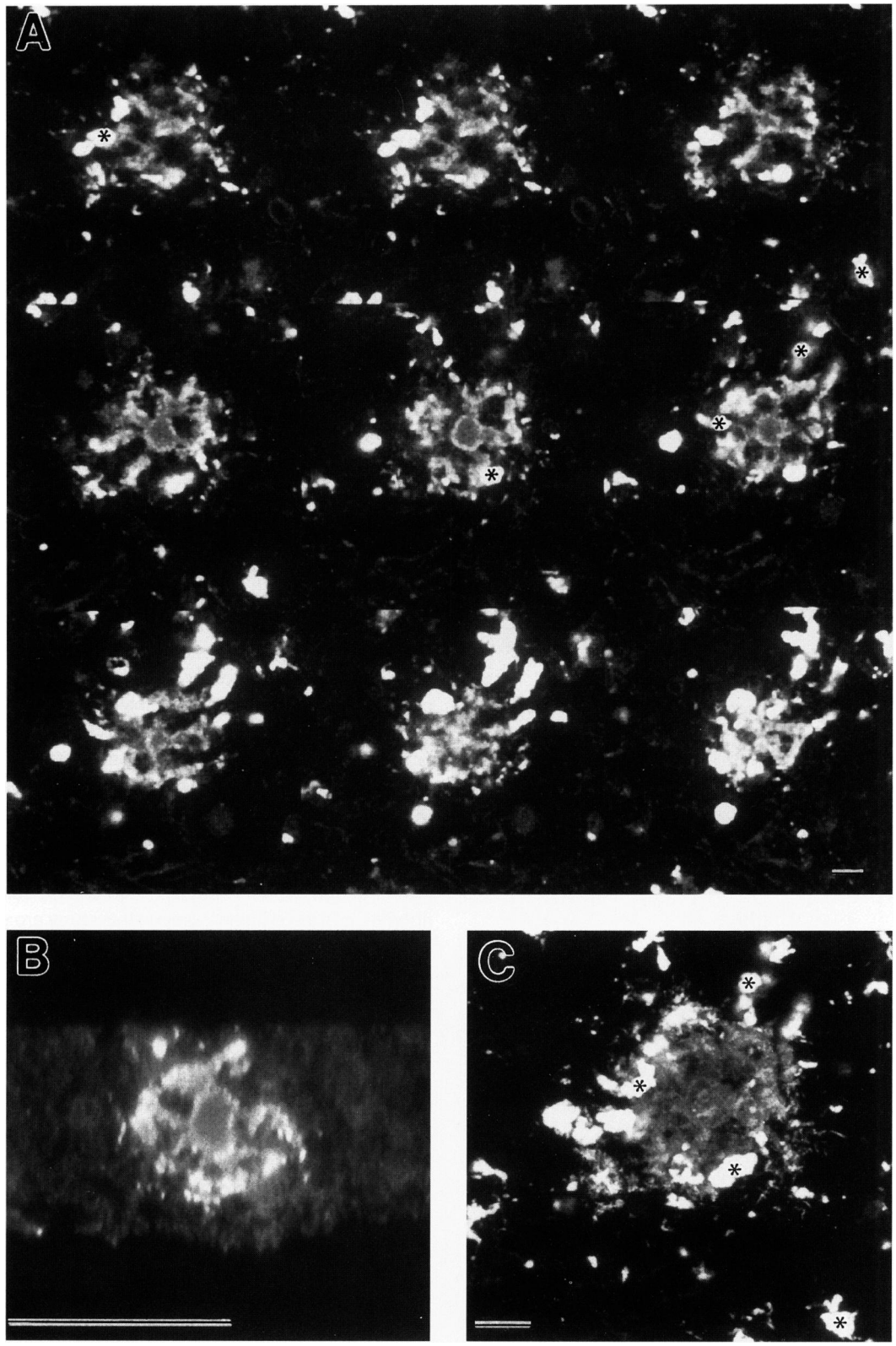
A
B
C

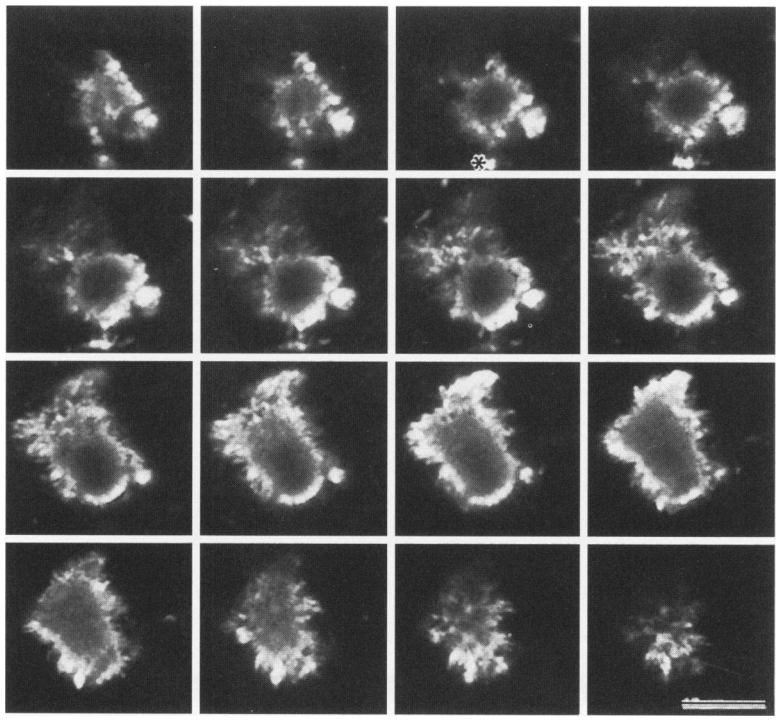

Figure 3. *Compact plaque in a 40 μm-thick frozen section immunostained with anti-Aβ antiserum 2332 and visualized with a TR-labeled secondary antibody. Fifty optical sections through the entire depth of a compact plaque at intervals of 0.21 μm were obtained in the CLSM. Sixteen of the sections are shown in this panel. Note the lightly immunostained center of the plaque and the immunostained jagged outer edges, which correspond to the perimeter of the so-called amyloid star identified in the electron microscope. See Discussion for further detail. Representative lipofuscin granules are marked by asterisks. Scale bar = 10 μm.*

Negative controls included 1) substituting spent supernatant of mouse myeloma cells (SP2) for one of the primary antibodies and 2) using the secondary fluorescently labeled antibody without an appropriate primary antibody. Additional control experiments included single label experiments conducted on sections using only one primary antibody and the appropriate secondary antibody tagged with FITC and TR. This strategy enabled us to vigorously monitor any evidence of "crosstalk" between the two channels of the confocal laser microscope (CLSM) (see also below).

Preparation and Staining of Paraffin Embedded Samples

Six μm-thick paraffin sections also were prepared from middle frontal cortex samples of patients 5 to 16 (Table 1). These sections were immunostained with anti-Aβ antisera (2332, UP107, SP28) and anti-tau antibodies (paired helical filament 1 (PHF1), T46, T3P) using the peroxidase anti-peroxidase (PAP) procedure and diaminobenzidine (DAB) as chromogen according to previously published methods.[26] Paraffin sections of middle frontal cortex from DS patients (nos. 17 to 23) also were immunostained with anti-tau (PHF1) and anti-Aβ antibodies (2332, 10D5) exactly as described.[26] In addition, 6 and 25 μm-thick paraffin sections from patients 5 to 23 were stained with thioS (see below) and Congo red according to Puchtler.[27] Different sets of sections were first immunostained with anti-Aβ antibodies in conjunction with the PAP method and counterstained with thioS or Congo red. The thioS staining protocol was adapted from J. Rogers (personal communication). Briefly, deparaffinized sections were hydrated and immersed for 1 hour in 4% neutral buffered formalin followed by rinses in tap water and PBS. Next, the sections were immersed in 0.05% $KMnO_4$ in PBS for 20 minutes. After rinsing in PBS, the sections were destained in O.2% $K_2S_2O_5$ and 0.2% oxalic acid in PBS for 3 minutes in the dark. After rinsing in PBS, sections were incubated in a 0.0125% solution of thioS in 40% ETOH and 60% PBS. Finally, the sections were differentiated in 50% ethanol in PBS, rinsed in PBS and coverslipped with antifade medium.[25]

Figure 2. *This is a frozen section from an AD patient that was immunostained with anti-Aβ antiserum and TR-labeled secondary antibody to reveal a classical plaque. Representative clumps of lipofuscin are marked by asterisks.* (A) *Nine CLSM images of a series of 20 optical sections obtained at 1-μm intervals are shown here. Scale bar = 10 μm.* (B) *Single optical section through the center of the same plaque in the z direction. The flat upper surface of the section is affixed to the glass slide, and the somewhat irregular lower surface of the section faces the objective. The section was covered with Crystal Mount without a coverslip. This image demonstrates that the 40 μm-thick section was completely penetrated by the antibodies. Scale bar = 40 μm.* (C) *In a composite of the first 13 optical planes of the same plaque the core is far less conspicuous. Stacking all 20 optical planes completely obscured the ring shape of the core of this plaque (data not shown). Scale bar = 10 μm.*

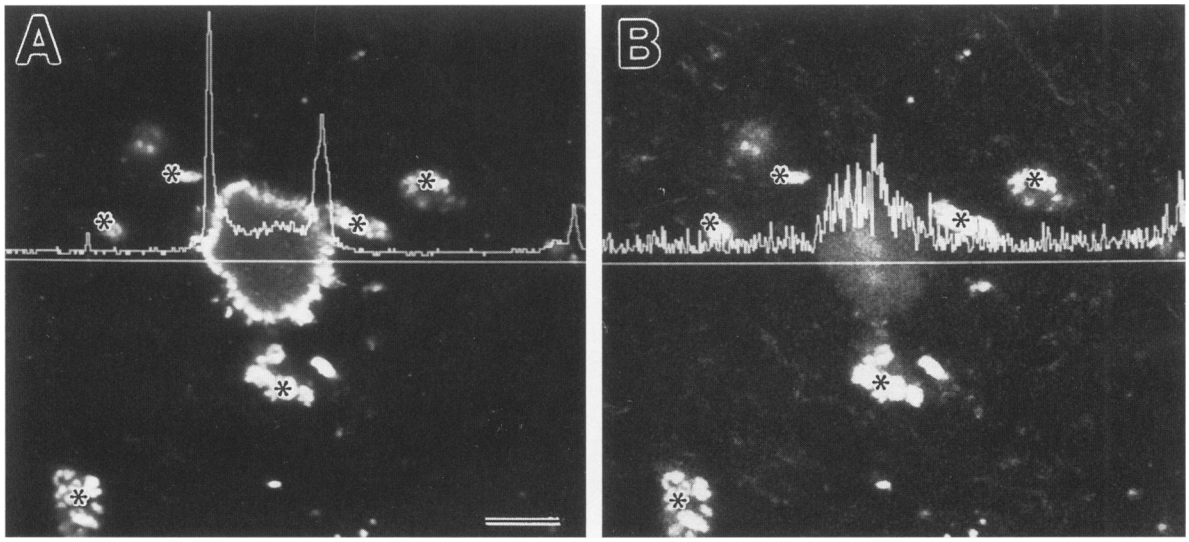

Figure 4. *A 40 μm-thick frozen section was immunostained with anti-Aβ antiserum 2332 and a TR-labeled secondary antibody. These two images of an immunostained compact plaque were recorded simultaneously in both channels from the same optical plane. Representative lipofuscin granules are marked by asterisks.* (**A**) *Immunofluorescently stained plaque core recorded by the first photomultiplier using TR filters.* (**B**) *The autofluorescent center of this plaque core was recorded simultaneously by the second photomultiplier using FITC filters. See also Discussion and Ref. 33. Scale bar = 10 μm.*

Brightfield and Fluorescence Microscopy

A Nikon FXA epifluorescence microscope equipped with a mercury bulb was used for brightfield and fluorescence observations. Standard filter cubes for FITC and FITC/TR were employed. In addition, a thioS filter cube (equipped with 405 nm exciter filter, 430 nm dichroic mirror, and 435 nm barrier filters) was used.

Confocal Microscopy and Quantitation

Fluorescently stained frozen sections were evaluated using a Leica CLSM (Heidelberg, Germany) equipped with a Leica Fluovert microscope and a krypton/argon ion laser. Using a 60X Nikon Planapo lens (numerical aperture 1.4), FITC and TR double-labeled preparations were recorded simultaneously in separate channels using a short pass 590 nm excitation filter, a double dichroic beam splitter (488/568 nm), and a bandpass 535 ± 15 nm barrier filter for FITC and a longpass 590 nm barrier filter for TR. Initial tests confirmed that there is negligible crosstalk between the FITC and TR signal with these filter settings. Measurements of fluorescently labeled plaques were performed using the Leica CLSM software. Briefly, the optical section showing the largest cross section through each anti-Aβ-immunostained plaque core was chosen and the largest inner diameter of circular plaque cores or the largest and smallest average inner diameter of elliptical plaque cores was obtained. The smallest width of the amyloid rim was also noted. From these data, the average diameter and rim width of plaque cores were calculated. Pixel intensities were computed along a line plotted within the image (see below).

Photography

Confocal images were photographed directly from the high resolution true color display monitor with a tripod mounted camera equipped with a flat field lens and Kodak T-MAX 100 film. Brightfield and fluorescent photo micrographs were taken with a Nikon FXA photo microscope using Kodak Technical Pan and T-MAX 100 films for bright field, and T-MAX 400 film for fluorescence.

Results

AD Patients

Optical sectioning by CLSM of plaque cores in classical and compact plaques immunostained with anti-Aβ antibodies showed strongly stained rims (Figure 1A) and weakly stained centers. Classical plaques consist of an amyloid core and a corona, while compact plaques are cores without coronas. The amyloid cores in both types of plaques appear to be identical in size and staining properties. The centers of these amyloid cores autofluoresced in the FITC channel (Figure 1 B). Similar "ring-shaped" plaque cores, although uncommon, can be found in preparations immunostained with the same antibodies

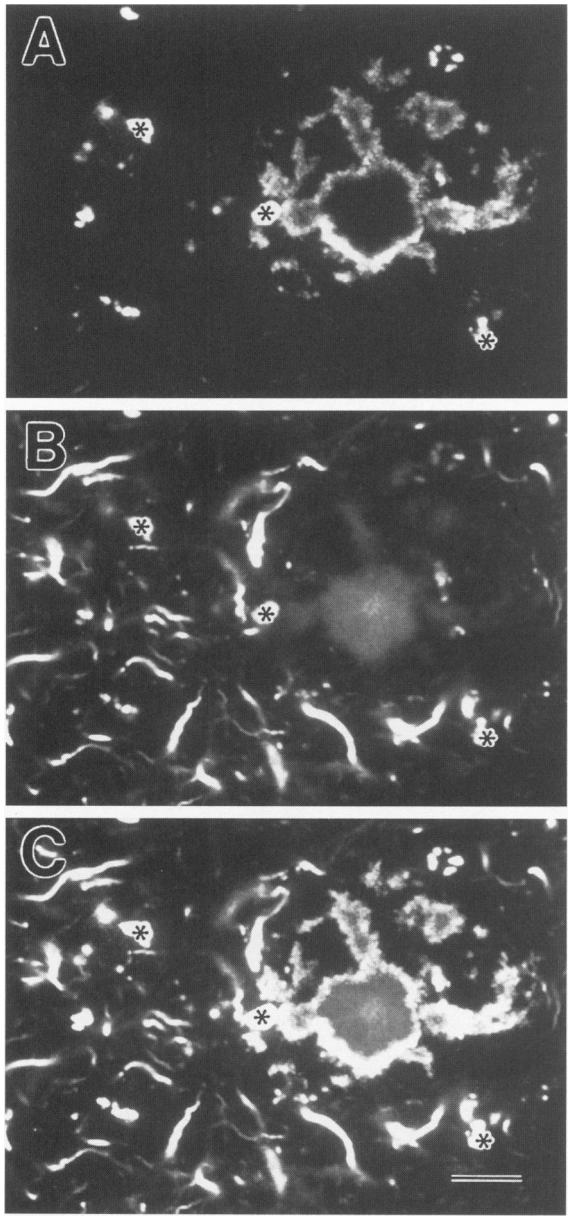

Figure 5. *This figure shows a compact plaque double-immunostained with anti-Aβ antibodies 2332 and PHF-tau antibody PHF1 visualized with TR and FITC-labeled secondary antibodies in a 40 μm-thick frozen section. Asterisks mark representative clumps of lipofuscin granules.* **A** *shows an image of a single optical plane obtained in the TR channel;* **B** *depicts a simultaneously acquired image of PHF1/FITC immunoreactive neuropil threads as well as the autofluorescent plaque center in the FITC channel. In* **C**, *the images from* **A** *and* **B** *are superimposed. Scale bar = 10 μm.*

using the PAP procedure and DAB (Figure 1 C). Serial optical sections demonstrated that plaque cores in classical plaques (Figure 2) and compact plaques (Figure 3) are immunoreactive hollow spheres. Measurements of the largest inner diameters of 45 optically sectioned plaque cores showed an average diameter of 8.8 μm (range, 2.4–16.2 μm). The narrow portions of immunoreactive rims measured 2.2 μm on the average (range, 1.1–5.7 μm). Using the Leica CLSM software, numerical values of pixel intensities along a line drawn through a plaque core immunostained with an anti-Aβ antiserum and a TR-labeled secondary antibody were recorded to a data file. Connecting these data points produced the graph in Figure 4, which showed that the immunostaining intensity within the plaque core center was slightly above background in the TR image. However, the autofluorescence of this center recorded in the FITC channel was more intense than the anti-Aβ immunostain. The pixel intensities also indicated that there was negligible background due the immunostaining procedure in the neuropil outside the plaques. In contrast, the FITC channel revealed considerable autofluorescent "background" due to widespread amyloid. In some instances, autofluorescent "stalks" extended from the autofluorescent cores. These "stalks" were also surrounded by an anti-Aβ antibody-immunoreactive rim (Figure 5). The autofluorescent centers also were evident in unstained frozen sections examined by the epifluorescent microscope using a FITC filter cube. With the thioS filter cube, a bluish fluorescence of the plaque core and plaque corona was apparent (data not shown). Plaque cores immunostained with anti-Aβ antibodies by the PAP method that also were counterstained with thioS or Congo red showed a fluorescent center or "Maltese cross" profile when viewed in the fluorescent microscope (Figure 6) or with crossed polarizers, respectively (data not shown). The interior of the plaque cores did not show any immunoreactivity to tau, PHF-tau, fetal tau, or glial fibrillary protein (see Table 1 for the antibodies used).

Figure 7 illustrates schematically that in 6 μm-thick sections hollow spheres with an outer diameter of 13 μm and a 2 μm-thick wall will frequently appear as disks. Only when the top and bottom of the spheres are not contained within the section will the unstained interior of the spheres appear as lighter centers in the disks. Thus, the ring-shaped plaque cores observed by optical sectioning using the CLSM can be seen in the light microscope only in fortuitously sectioned plaques of appropriate size that are located exactly in the center of the 6 μm-thick tissue section. This explains why only a portion of the plaque cores immunostained using the PAP method and DAB showed centers stained with thioS or Congo red.

Classical and compact plaques predominate in infragranular layers of AD frontal cortices and are also found interspersed among large numbers of diffuse Aβ deposits in supragranular layers of frontal cortex.

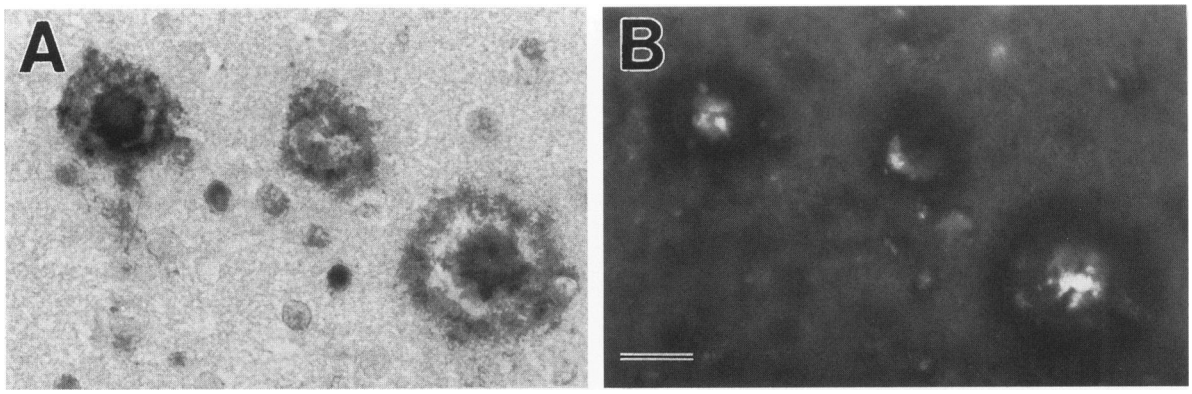

Figure 6. *A 6 μm-thick paraffin section was immunostained with antiserum 2332 and the PAP procedure and counterstained with thioS.* (**A**) *Brightfield photomicrograph showing three plaques. Classical plaques with spherical cores are shown on the left and right, while the plaque in the middle has a questionable center.* (**B**) *When the same plaques were photographed under fluorescent illumination and a thioS filter set, the two classical plaques displayed a strongly fluorescent core. The middle plaque contains autofluorescent lipofuscin granules that could be resolved by focusing up and down. Scale bar = 20 μm.*

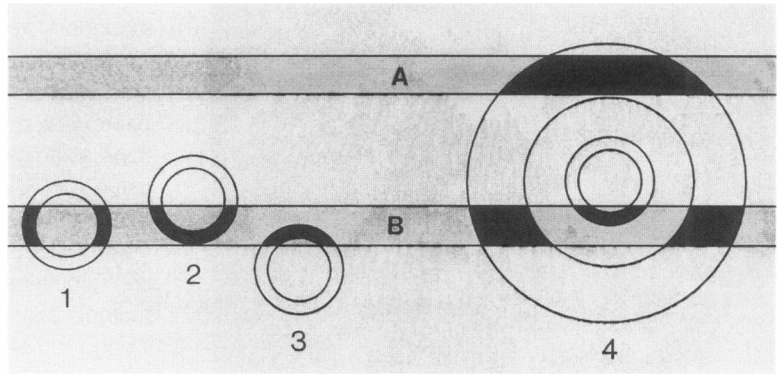

Figure 7. *This diagram illustrates the relationship between section thickness and plaque diameter. A schematic drawing of two 6 μm-thick tissue sections* (**A**) *and* (**B**) *and three compact plaques (1, 2, and 3; outer diameter, 14 μm; inner diameter, 10 μm) and a mature plaque (4; outer diameter, 50 μm; the core is the same size as the compact plaques). In a single section compact plaque 1 will appear ring-shaped, whereas compact plaques 2 and 3 will appear disk-shaped. The classical plaque on the right (4) will appear different in section* **A** *versus* section **B**. *However, thick tissue sections contain larger portions of plaques. Moreover, optical z-sections generated in the confocal microscope easily confirm whether a given plaque is located in the middle of the tissue section or whether the plaque was cut and only part of it is contained in the tissue section. Compare with Figure 2 C.*

In this brain region, the number of classical and compact plaques is highly variable among AD patients. The thioS-positive and anti-Aβ-negative centers were observed in every compact plaque and in every classical plaque with a clearly delimited core. Fibrous plaques are uncommon in most AD brains and will be described in the next paragraph on DS patients, in whom they were much more numerous.

Down's Syndrome Patients

Classical and compact plaques with immunoreactive rims and thioS-positive centers as described in AD brains were extremely rare in the middle frontal cortex samples of the DS brains studied. Immunostaining of DS plaques using anti-Aβ antibodies and PAP with DAB showed accumulations of irregular patchy Aβ deposits similar to those seen in AD plaques, while thioS staining of adjacent sections showed a subset of plaques composed predominantly of thioS-positive fibrous material (Figure 8, A and B). Fibrous, thioS-positive plaques were variable in appearance, and we observed them in six of the seven DS patients studied here. Most plaques that resembled classical plaques in DS patients showed ill-defined cores (Figure 8A). These poorly delimited cores were immunoreactive with anti-Aβ antibodies as well as thioS positive. Only rarely were plaques with this fibrous morphology found in thioS-stained sections of AD patients (Figure 8C). However, more frequently AD plaques showed less distinct fibrous components after optical sectioning by CLSM (Figure 8D). Many plaques in the frontal cortex of the AD and DS patients were lightly stained with thioS, and some of them contained thioS-positive dystrophic neurites as illustrated in the lower right panel of Figure 8A. As demonstrated in Figure 9, some plaques in DS brains were strongly Aβ immunoreactive as well as strongly thioS positive.

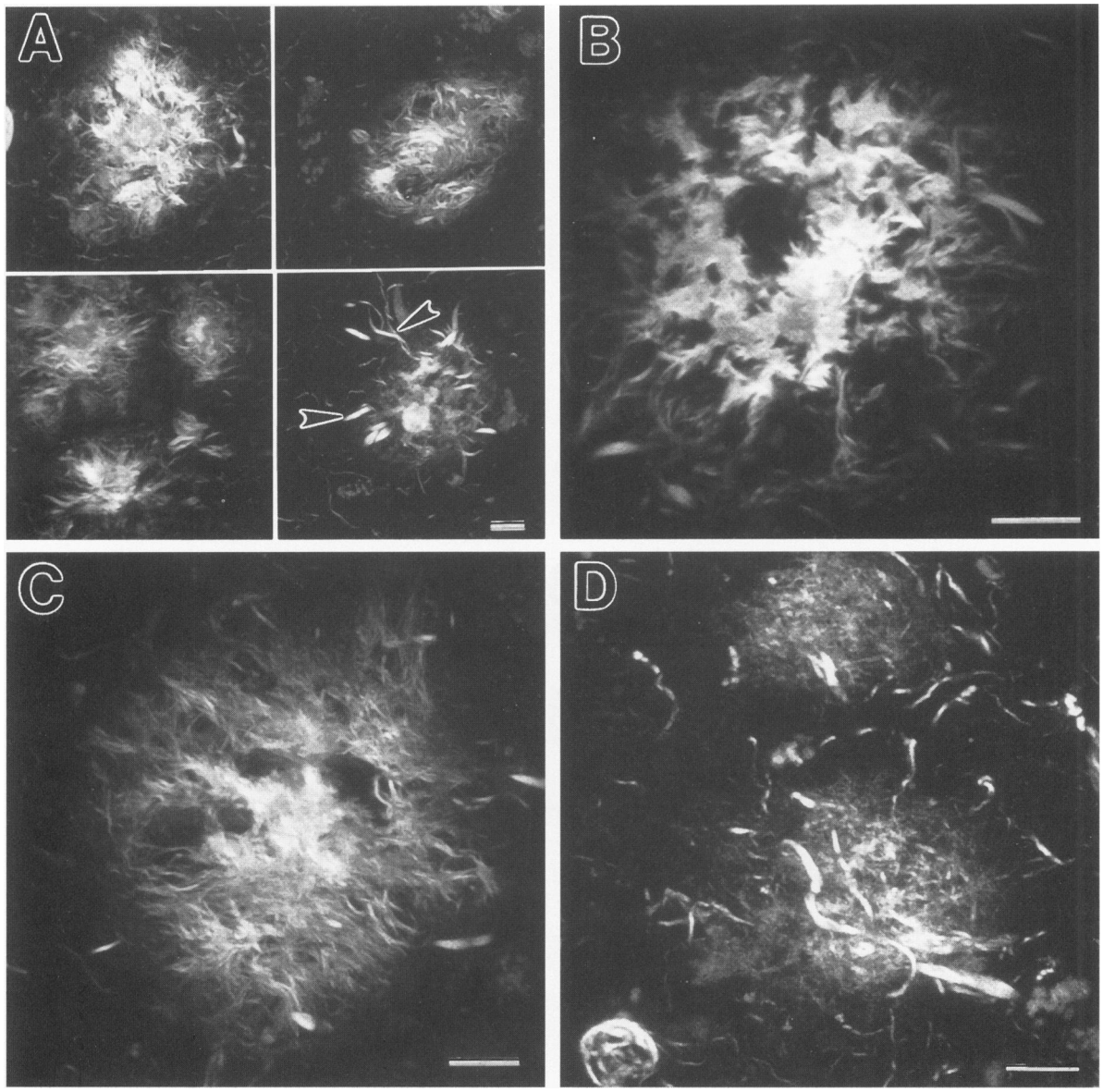

Figure 8. *Fibrous plaques are shown in these 25 μm-thick paraffin sections of frontal cortex that were stained with thioS and viewed with FITC filter settings in the CLSM. Each photograph represents a composite of 8 to 12 optical sections.* (**A**) *Varied morphologies of fibrous plaques of a DS patient (upper panels, lower left panel). The lower right panel depicts a plaque containing dystrophic neurites in a DS brain. Dystrophic neurites are also stained with thioS. These membrane-bound dystrophic neurites are sharply delineated* (**arrowheads**), *and this distinguishes them from the less well delineated extracellular fibrous Aβ components.* (**B**) *Higher magnification of a fibrous plaque of a DS brain.* (**C**) *A fibrous plaque from an AD brain. This plaque is similar to the numerous fibrous plaques in DS brains. However, fibrous plaques are rare in AD brains.* (**D**) *Many plaques in AD brains appear amorphous when viewed in epifluorescence but by superimposing 12 optical sections some fibrous components became apparent. In addition, these two plaques contain dystrophic neurites. All scale bars = 10 μm.*

However, only occasionally were some fibrous components detected in immunostained plaques, and never to the extent seen in thioS-stained preparations as illustrated in Figure 10. Noteworthy are the defined borders of these immunostained plaques, which contrast with the poorly delimited thioS-positive fibrous plaques (compare Figures 8 and 10).

Fibrous plaques were prominent in six of the seven DS patients studied. One 53-year-old DS patient (no. 17) had conspicuously fewer plaques in the frontal cortex than did the other DS patients, although plaque numbers in this patient still exceeded the National Institute on Aging Consensus Criteria for the diagnosis of AD.[24] ThioS-stained plaques in this pa-

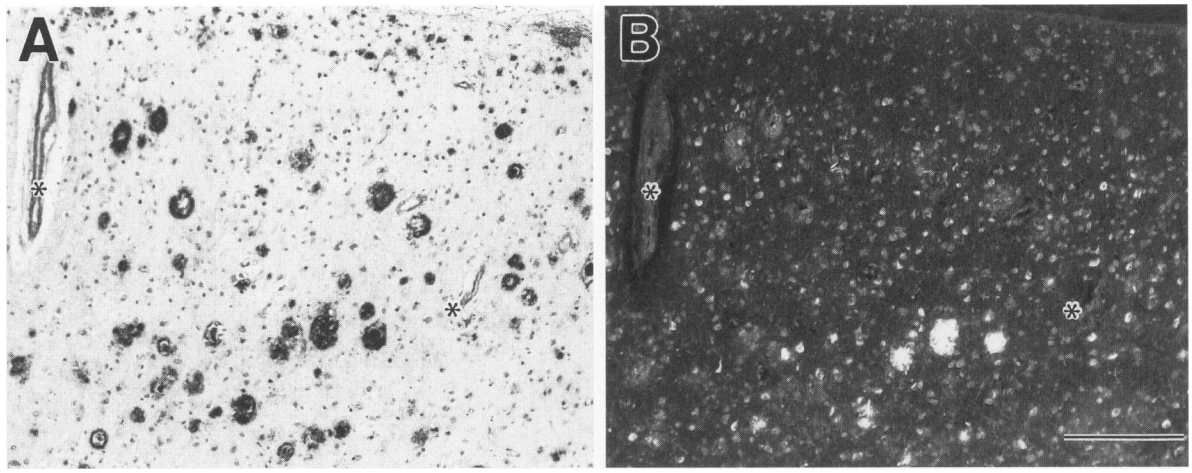

Figure 9. *Two adjacent 6 μm-thick paraffin sections of a DS brain were immunostained with anti-Aβ antiserum 2332 using PAP and DAB* (A) *and thioS* (B). *Asterisks mark the same blood vessels in both sections. Only three of numerous immunostained plaques are brightly fluorescent in the thioS-stained section. Scale bar = 100 μm.*

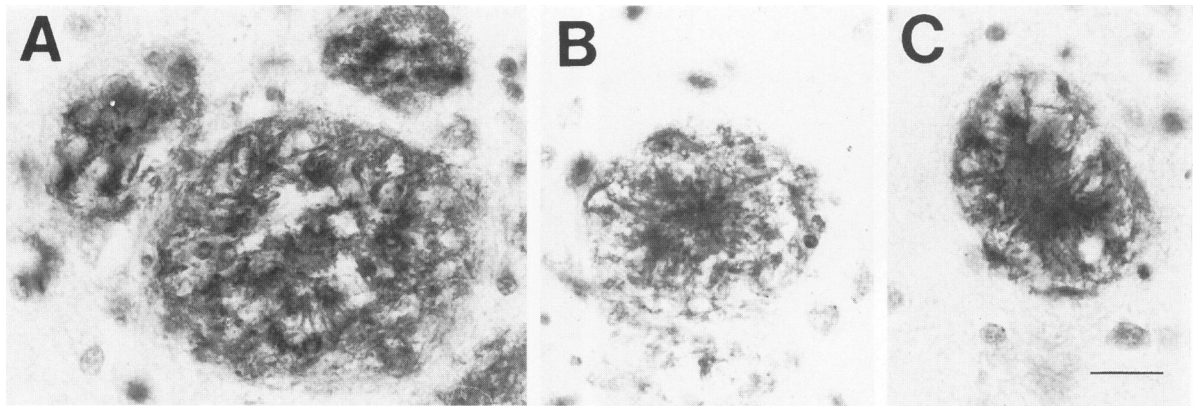

Figure 10. *Six μm-thick paraffin sections of DS frontal cortex were immunostained with anti-Aβ antiserum 2332 using PAP and DAB and counterstained with hematoxylin. In a subset of immunostained DS plaques some fibrous structures are discernable. Scale bar = 20 μm.*

tient did not appear fibrous as in the other DS patients. Instead, they resembled the amorphous or very faint staining often seen in plaques of AD patients. Interestingly, this retarded patient did not show further mental decline before her death.

Discussion

In this study, we demonstrate a form of amyloid that is thioS positive, but only weakly or not at all immunoreactive with anti-Aβ antibodies. This thioS-positive amyloid was seen commonly in the center of spherical amyloid cores of classical and compact plaques in AD brains and in fibrous plaques in DS brains. The "spherical" amyloid cores described in this study are referred to as amyloid stars by electron microscopists, and they have been shown repeatedly to be composed entirely of fibrillar amyloid.[28–31] Thus, our data suggest that amyloid fibrils in the peripheral region of the amyloid star where bundles of amyloid fibrils interdigitate with microglial processes are strongly immunoreactive with anti-Aβ antibodies. In contrast, amyloid fibrils in the center of the amyloid star are far less Aβ immunoreactive, but they are strongly thioS positive. This raises the possibility that antibodies cannot penetrate the densely packed amyloid fibrils in the center of the amyloid star while thioS, a much smaller molecule, has access. This is unlikely, given that cut surfaces of these amyloid cores also remain unstained as demonstrated in Figure 1C. In addition only the centers of these cores are autofluorescent, indicating a difference in the molecular composition of the center and the rim of the cores (Figure 1, A and B).

Although many classical plaques (eg, those with core and corona) were found in DS brains, the great majority of these plaques differ from their counterparts in AD brains morphologically and in their staining properties with anti-Aβ antibodies and thioS. This

implies that there may be differences in the molecular composition of these plaques as well. Plaque cores in DS brains were irregular and often larger than the ring-shaped cores in AD plaques as reported previously.[32] Moreover, these irregular cores in DS plaques are immunoreactive with anti-Aβ antibodies as well as thioS positive in contrast to the spherical AD plaque cores (see above). ThioS-positive fibrous plaques are uncommon in AD patients but they were numerous in most of the DS brains studied here. Occasionally some fibrous components are present in anti-Aβ immunostained plaques of AD; however, patchy or amorphous immunostaining is more common. This indicates that most of the thioS fibrous components of these plaques are made up of a form of amyloid that is not immunoreactive with anti-Aβ antibodies. Notably, descriptions of thioS-positive fibrous amyloid plaques (termed caput medusae) as well as their autofluorescence with UV illumination had been reported earlier.[33,34] Classical and compact plaques occur mainly in AD and control patients aged 70 years and older.[35] All DS patients in this study were younger than 70 years old, and this might explain the virtual lack of classical and compact plaques with spherical cores in the brains of these patients.

These findings raise questions concerning the identity of the thioS-positive and non-Aβ-immunoreactive material in the structures described here. One possibility is that this material is unrelated to Aβ. For example, it could be amyloid P, which is thioS positive and has been found in amyloid plaques.[36,37] Alternatively, this material could represent Aβ that is altered in different ways.[38] For example, studies conducted with monoclonal antibodies specific to the 1–40 and the 1–42(43) amino acid forms of Aβ have shown that Aβ 1–42(43) is found in larger numbers of plaques than Aβ 1–40 but that Aβ 1–40 is more frequently found in cored than in uncored plaques.[39,40] Thus, proteolysis could modify the immunological properties of Aβ peptides in plaques. Further, other modifications of amino acids in the Aβ peptide have been described in the brains of AD and DS patients, and a recent study showed that modified forms of Aβ may not be recognized by antibodies raised to the unmodified Aβ peptides.[41] Alternatively, glycation, polymerization, or other modifications mediated by plaque associated elements such as microglia may alter Aβ, thereby rendering thioS-positive Aβ non-immunoreactive with anti-Aβ antibodies.[42–44] One must also consider the possibility that thioS binds to one of the many other plaque-associated proteins that are not typically regarded as amyloidogenic.[45–47] Finally, thioS may bind to some forms of Aβ peptides only when they are associated with one of these proteins. For example, Snow et al.[48] recently showed that synthetic Aβ injected into rat brain consistently formed thioS and Congo red-positive deposits only when heparan sulfate proteoglycans were added to the injectate. Given that Aβ-immunoreactive plaques occur commonly in AD as well as during normal aging, it is important to identify those forms of Aβ that are most closely linked to the dementia and the degeneration of selective groups of neurons in AD.

Acknowledgments

We thank Dr. B. Frangione for the antiserum SP28, and Mr. J. DiRienzi for assisting with the collection of the tissue samples. We also thank Dr. Steve Arnold for reading the manuscript and his helpful comments. Finally, we are grateful to all the families who enabled us to carry out this work by donating tissues.

References

1. Glenner GG: Alzheimer's disease: its proteins and genes. Cell 1988, 52:307–308
2. Bush AI, Beyreuther K, Masters CL: βA4 amyloid protein, and its precursor in Alzheimer's disease. Pharmac Ther 1992, 56:97–117
3. Shoji M, Golde TE, Ghiso J, Cheung TT, Estus S, Shaffer LM, Cai X-D, McKay DM, Tintner R, Frangione B, Younkin SG: Production of the Alzheimer amyloid β protein by normal proteolytic processing. Science 1992, 258:126–129
4. Wertkin A, Turner RS, Pleasure SJ, Golde TE, Younkin SG, Trojanowski JQ, Lee VM-Y: Human neurons derived from a teratocarcinoma cell line express solely the 695-amino acid amyloid precursor protein and produce intracellular β-amyloid or A4 peptides. Proc Natl Acad Sci USA 1993, 90: 9513–9517
5. Haass C, Schlossmacher MG, Hung AY, Vigo-Pelfrey C, Mellon A, Ostaszewski BL, Lieberburg I, Koo EH, Schenk D, Teplow DB, Selkoe DJ: Amyloid β-peptide is produced by cultured cells during normal metabolism. Nature 1992, 359:322–325
6. Kuentzel SL, Ali SM, Altman RA, Greenberg BD, Raub TJ: The Alzheimer β-amyloid protein precursor/protease nexin-II is cleaved by secretase in a trans-Golgi secretory compartment in human neuroglioma cells. Biochem J 1993, 295:367–378
7. Maruyama K, Terakado K, Usami M, Yoshikawa K: Formation of amyloid-like fibrils in COS cells overexpressing part of the Alzheimer amyloid protein precursor. Nature 1990, 347:566–569
8. De Strooper B, Umans L, Van Leuven F, Van Den Berghe H: Study of the synthesis and secretion of normal and artificial mutants if murine amyloid precursor

protein (APP): cleavage of APP occurs in a late compartment of the default secretion pathway. J Cell Biol 1993, 121:295–304
9. Sambamurti K, Shioi JP, Anderson JP, Pappolla MA, Robakis Nk: Evidence for intracellular cleavage of the Alzheimer's amyloid precursor in PC12 cells. J Neurosci Res 1992, 33:319–329
10. Ikeda S-I, Allsop D, Glenner GG: Morphology and distribution of plaque and related deposits in the brains of Alzheimer's disease and control cases. An immunohistochemical study using amyloid β-protein antibody. Lab Invest 1989, 60:113–122
11. Yamaguchi H, Hirai S, Morimatsu M, Shoji M, Ihara Y: A variety of cerebral amyloid deposits in the brains of Alzheimer-type dementia demonstrated by β protein immunostaining. Acta Neuropathol 1988, 76:541–549
12. Wisniewski HM, Bancher C, Barcikowska M, Wen GY, Currie J: Spectrum of morphological appearance of amyloid deposits in Alzheimer's disease. Acta Neuropathol 1989, 78:337–347
13. Majocha RE, Benes FM, Reifel JL, Rodenrys AM, Marotta CA: Laminar-specific distribution and infrastructural detail of amyloid in the Alzheimer disease cortex visualized by computer-enhanced imaging of epitopes recognized by monoclonal antibodies. Proc Natl Acad Sci USA 1988, 85:6182–6186
14. Pappolla MA, Omar RA, Vinters HV: Image analysis microspectroscopy shows that neurons participate in the genesis of a subset of early primitive (diffuse) senile plaques. Am J Pathol 1991, 139:599–607
15. Pappolla MA, Omar RA, Sambamurti K, Anderson JP, Robakis Nk: The genesis of the senile plaque. Further evidence in support of its neuronal origin. Am J Pathol 1992, 141:1151–1159
16. Giaccone G, Tagliavini F, Linoli G, Bouras C, Frigerio L, Frangione B, Bugiani O: Down patients: extracellular preamyloid deposits precede neuritic degeneration and senile plaques. Neurosci Lett 1989, 97:232–238
17. Ikeda S-I, Yanagisawa N, Allsop D, Glenner GG: Evidence of amyloid β-protein immunoreactive early plaque lesions in Down's syndrome brains. Lab Invest 1989, 61:133–137
18. Mann DMA, Brown A, Prinja D, Davies CA, Landon M, Masters CL, Beyreuther K: An analysis of the morphology of senile plaques in Down's syndrome patients of different ages using immunocytochemical and lectin histochemical techniques. Neuropathol Appl Neurobiol 1989, 15:317–329
19. Allsop D, Haga S-I, Haga C, Ikeda S-I, Mann DMA, Ishii T: Early senile plaques in Down's syndrome brains show a close relationship with cell bodies of neurons. Neuropathol Appl Neurobiol 1989, 15:531–542
20. Verga L, Frangione B, Tagliavini F, Giaccone G, Migheli A, Bugiani O: Alzheimer patients and Down patients: cerebral preamyloid deposits differ ultrastructurally and histochemically from the amyloid of senile plaques. Neurosci Lett 1989, 105:294–299
21. Mann DMA, Esiri MM: The pattern of acquisition of plaques and tangles in the brains of patients under 50 years of age with Down's syndrome. J Neurol Sci 1989, 89:169–179
22. Barcikowska M, Wisniewski HM, Bancher C, Grundke-Iqbal I: About the presence of paired helical filaments in dystrophic neurites participating in the plaque formation. Acta Neuropathol 1989, 78:225–231
23. Duyckaerts C, Delaere P, Poulain V, Brion J-P, Hauw J-J: Does amyloid precede paired helical filaments in the senile plaque? A study of 15 cases with graded intellectual status in aging and Alzheimer disease. Neurosci Lett 1988, 91:354–359
24. Khachaturian ZS: Diagnosis of Alzheimer's disease. Arch Neurol 1985, 42:1097–1105
25. Sherman H, Murray JM, DiLullo C: Confocal microscopy: an overview. Biotechniques 1989, 7:154–163
26. Schmidt ML, DiDario AG, Lee VM-Y, Trojanowski JQ: An extensive neocortical network of PHFτ-rich dystrophic neurites permeates nearly all neuritic and diffuse plaques in the Alzheimer disease brain. FEBS Lett 1994, 344:69–73
27. Puchtler H, Sweat F, Levine M: On the binding of Congo red by amyloid. J Histochem Cytochem 1962, 10:355–364
28. Wisniewski HM, Wegiel J: Spatial relationships between astrocytes and classical plaque components. Neurobiol Aging 1991, 12:593–600
29. Wisniewski HM, Vorbrodt AW, Wegiel J, Morys J, Lossinsky AS: Ultrastructure of the cells forming amyloid fibers in Alzheimer disease and scrapie. Am J Med Genet, Suppl 1990, 7:287–297
30. Wegiel J, Wisniewski HM: The complex of microglial cells and amyloid star in three-dimensional reconstruction. Acta Neuropathol 1990, 81:116–124
31. Wisniewski HM, Wegiel J, Wang KC, Kujawa M, Lach B: Ultrastructural studies of the cells forming amyloid fibers in classical plaques. Can J Neurol Sci 1989, 16: 535–542
32. Allsop D, Kidd M, Landon M, Tomlinson A: Isolated senile plaque cores in Alzheimer's disease and Down's syndrome show differences in morphology. J Neurol Neurosurg Psych 1986, 49:886–892
33. Schwartz P: Amyloidosis. Cause, and manifestation of senile deterioration. Springfield, Illinois, C. C. Thomas, 1970
34. Motte J, Williams RS: Age-related changes in the density and morphology of plaques and neurofibrillary tangles in Down syndrome brain. Acta Neuropathol 1989, 77:535–546
35. Ohgami T, Kitamoto T, Shin R-W, Kaneko Y, Ogomori K, Tateishi J: Increased senile plaques without microglia in Alzheimer's disease. Acta Neuropathol 1991, 81:242–247
36. Pepys MB, Rademacher TW, Amatayakul-Chantler S, Williams P, Noble GE, Hutchison WL, Hawkins PN, Nelson SR, Gallimore JR, Herbert J, Hutton T, Dwek RA: Human serum amyloid P component is an invari-

ant constituent of amyloid deposits and has a uniquely homogeneous glycostructure. Proc Natl Acad Sci USA 1994, 91:5602–5606
37. Kalaria RN, Galloway PG, Perry G: Widespread serum amyloid P immunoreactivity in cortical amyloid deposits and the neurofibrillary pathology of Alzheimer's disease and other degenerative disorders. Neuropathol Appl Neurobiol 1991, 17:189–201
38. Mori H, Takio K, Ogawara M, Selkoe D J: Mass spectrometry of purified amyloid β protein in Alzheimer's disease. J Biol Chem 1992, 267:17082–17086
39. Suzuki N, Iwatsubo T, Odaka A, Ishibashi Y, Kitada C, Ihara Y: High tissue content of soluble β1–40 is linked to cerebral amyloid angiopathy. Am J Pathol 1994, 145:452–460
40. Iwatsubo T, Odaka A, Suzuki N, Mizusawa H, Nukina N, Ihara Y: Visualization of Aβ42(43)-positive and Aβ40-positive senile plaques with end-specific Aβ-monoclonal antibodies: evidence that an initially deposited Aβ species is Aβ1–42(43). Neuron 1994, 13: 45–53
41. Saido TC, Iwatsubo T, Mann DMA, Shimada H, Ihara Y, Kawashima S: Dominant and differential deposition of distinct β-amyloid peptide species, $A\beta_{N3(pE)}$, in senile plaques. Neuron 1995, 14:1–20
42. El Hachimi KH, Foncin J-F: Do microglial cells phagocyte the β/A4-amyloid senile plaque core of Alzheimer disease? C R Acad Sci 1994, 317:445–451
43. Cras P, Kawai M, Siedlak S, Mulvihill P, Gambetti P, Lowery D, Gonzales-DeWhitt PA, Greenberg B, Perry G: Neuronal and microglial involvement in β-amyloid protein deposition in Alzheimer's disease. Am J Pathol 1990, 137:241–246
44. Perlmutter LS, Scott SA, Chui HC: The role of microglia in the cortical neuropathology of Alzheimer disease. Bull Clin Neurosci 1991, 56:120–130
45. Schmidt ML, DiDario AG, Otvos L Jr, Hoshi N, Kant A, Lee VM-Y, Trojanowski JQ: Plaque-associated neuronal proteins: a recurrent motif in neuritic amyloid deposits throughout diverse cortical areas of the Alzheimer's disease brain. Exp Neurol 1994, 130:311–322
46. Trojanowski JQ, Shin R-W, Schmidt ML, Lee VM-Y: Relationship between plaques, tangles and dystrophic processes in Alzheimer's disease. Neurobiol Aging 1995, 16:335–345
47. Selkoe D: Physiological production of the β-amyloid protein and the mechanism of Alzheimer's disease. TINS 1993, 16:403–409
48. Snow AD, Sekiguchi R, Nochlin D, Fraser P, Kimata K, Mizutani A, Arai M, Schreier WA, Morgan DG: An important role of heparan sulfate proteoglycan (perlecan) in a model system for the deposition and persistence of fibrillar Aβ-amyloid in rat brain. Neuron 1994, 12:219–234
49. Hyman BT, Tanzi RE, Marzloff K, Bartour R, Schenk D: Kunitz protease inhibitor-containing amyloid β protein precursor immunoreactivity in Alzheimer's disease. J Neuropathol Exp Neurol 1992, 51:76–83
50. Bramblett GT, Goedert M, Jakes R, Merrick SE, Trojanowski JQ, Lee VM-Y: Abnormal tau phosphorylation at ser396 in Alzheimer's disease recapitulates development and contributes to reduced microtubule binding. Neuron 1993, 10:1089–1099
51. Greenberg SG, Davies P: A preparation of Alzheimer paired helical filaments that displays distinct τ proteins by polyacrylamide gel electrophoresis. Proc Natl Acad Sci USA 1990, 87:5827–5831
52. Arai H, Lee VM-Y, Otvos L,Jr., Greenberg BD, Lowery DE, Sharma SK, Schmidt ML, Trojanowski JQ: Defined neurofilament, tau and β-amyloid protein epitopes distinguish Alzheimer from non-Alzheimer senile plaques. Proc Natl Acad Sci USA 1990, 87:2249–2253
53. Ghiso J, Wisniewski T, Vidal R, Rostagno A, Frangione B: Epitope map of two polyclonal antibodies that recognize amyloid lesions in patients with Alzheimer's disease. Biochem J 1992, 282:517–522